Receiver Output Stability Analysis
Part I: Concepts
Whitham D. Reeve

I-1. Introduction

The emissions received from many celestial radio sources are indistinguishable from the random noise generated by the receiver system itself, in fact they can be substantially lower than the receiver noise. The effect of the celestial source is to increase the already existing noise by a small amount. Detecting such small changes requires that the observed power is averaged or integrated over time. However, increasing detection sensitivity by averaging is only effective for certain types of noise. In particular, the receiver noise must be Gaussian or close to Gaussian. Gaussian noise is a category of noise also called *white frequency modulation*, or white FM, noise and often colloquially called *pure* noise. White FM noise has a flat spectrum over the frequency range of interest and, in the time domain the noise has random amplitudes with zero average (figure 1-1).
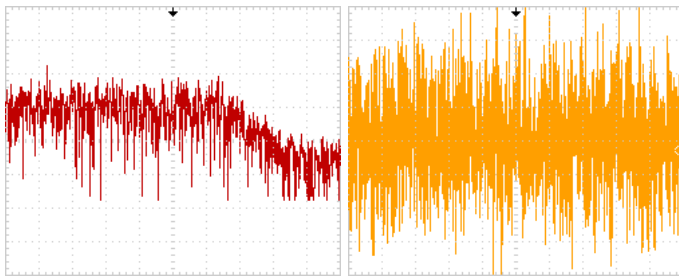

Figure 1-1 ~ Left: *Frequency domain* oscilloscope screenshot of white FM noise produced by a noise generator that has been bandlimited to 15 MHz. The trace was produced by the fast Fourier Transform function with frequency base of 2.5 MHz/div (note dropoff to right of 6th division). Right: *Time domain* oscilloscope screenshot of same noise with timebase of 5.0 µs/div. Images © 2016 W. Reeve

During relatively long observations, the receiver's averaged output eventually starts to drift and different types of non-Gaussian noise dominate the output. Beyond this point continued averaging does not reduce the noise fluctuation and instead may increase it, thus reducing rather than increasing the system sensitivity. The problem for a given system and set of conditions is to determine the longest averaging interval that is effective for reducing the noise effects.

Amateur radio astronomers often use total power receivers because of their relative simplicity. The stability of a total power receiver determines how long its output may be averaged. Receiver stability can be measured and analyzed by terminating its RF input with a resistive termination or stable noise generator, regularly sampling the receiver output and then computing and plotting a statistical property of the samples called the Allan Deviation.

In Part I of this paper I discuss the basic characteristics of total power receivers and the Allan Deviation calculations that may be used to analyze receiver stability. In Part II I discuss measurement methods and provide stability measurements for several common receivers used in amateur radio astronomy. I also include similar measurements for soundcards because they are used with analog narrowband receivers and can potentially dominate the statistical properties of the output data. Part II focuses on receivers operating in the high frequency (HF) band, particularly the upper portion from 15 to 30 MHz. However, the concepts and measurement methods apply to any total power receiver at any frequency. The information presented here may help readers measure the maximum averaging times for their receiver systems.

This paper builds on two papers by C. Monstein published in **Radio Astronomy** in which he discussed statistical measurements of the Callisto instrument's output characteristics in an unconditioned environment [Monstein12] and in a temperature stable environment [Monstein14]. The Callisto is a frequency-agile (channelized), total power receiver.

I-2. Total Power Receiver Characteristics

A total power receiver, or *radiometer*, measures the average noise power received across its bandwidth and over its integration time. This type of receiver may be based on an analog superheterodyne (superhet) or direct conversion (zero IF) architecture, a radio frequency (RF), intermediate frequency (IF) or audio frequency (AF) sampling software defined radio (SDR) receiver, or a combination. An RF sampling SDR receiver will be used to illustrate the key attributes of a total power receiver: Noise bandwidth B and output time constant τ (figure 1-2).
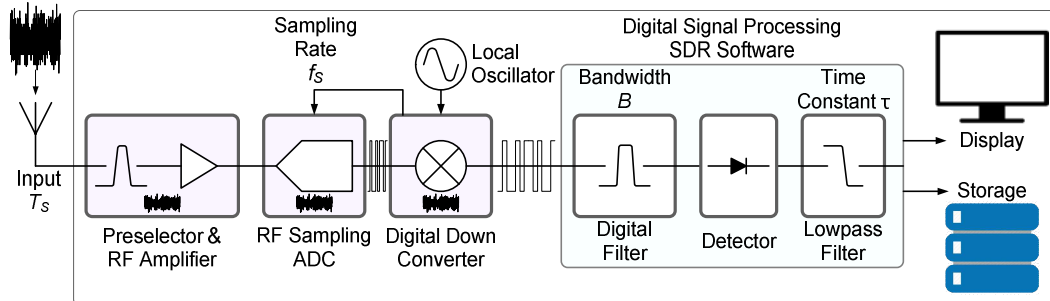

Figure 1-2 ~ Simplified diagram of an RF sampling SDR used as a total power receiver (controller components not shown). The received RF input has equivalent system noise temperature T_S, which includes not only the desired emissions and other noise received by the antenna but also noise from each receiver hardware stage referred to the input; of these, the first RF amplifier is the most important in terms of noise performance. The analog RF is digitized in the analog-digital converter with a sampling rate f_S at least twice the bandwidth being digitized. The ADC output bit-stream is reduced to a lower rate in the digital down-converter before being passed to the computer. The digitized data is processed by digital signal processing functions in the SDR software. The bandwidth B is determined by the digital filter and the time constant τ is determined by the sampling interval of a digital lowpass smoothing filter or integrator. Images © 2017 W. Reeve

The receiver RF input is filtered (band-limited) and then digitized by an RF sampling analog-digital converter (ADC). The rate of the digitized data from the ADC may be reduced by decimation in a digital down-converter (DDC) before being passed to the receiver output. The output typically is a digitized In-phase, I, and quadrature phase, Q, signal that is processed by the receiver's associated software to provide the equivalent of detection and to produce plots and store the data. A computer, typically a PC, is an essential part of an SDR receiver. The noise bandwidth of the digitized RF typically is determined by the filtering functions in the SDR software running on the computer. The filter bandwidth can range from a few Hz to a several tens of MHz. The processed data is sampled with the equivalent of a smoothing filter, which determines the output time constant τ . The smoothing filter bandwidth can range from close to zero frequency (dc) to a few Hz.

An IF sampling SDR receiver uses superheterodyne techniques to convert the RF input to a lower IF for sampling by a technically less demanding and cheaper ADC. In contrast to the RF and IF sampling SDR receivers, many

narrowband superhet or direct conversion receivers have an analog AF output that is connected to an audio ADC for digitization. The ADC usually is part of a PC soundcard and its output data is processed to produce a plot of output power over time. The analog receiver audio output bandwidth can be from a few hundred Hz to 15 kHz, depending on the receiver and its settings. The soundcard itself may be capable of several tens or a couple hundreds of kHz bandwidth. Some inexpensive SDR receivers have built-in soundcards that are able to process almost 200 kHz bandwidth and use a USB port for connection to a PC. The software on the PC processes the audio and provides the equivalent of detection and a smoothing filter with the desired time constant.

When a receiver's RF input is connected to a 50 ohm resistance termination (figure 1-3.a) or a noise generator (figure 1-3.b), the input noise power or noise temperature is a fixed value. The resistance termination has a noise temperature of 290 kelvin whereas, for the measurements described in this paper, the noise generator is set to a much higher noise temperature in the range 40 000 to 50 000 K. The advantage of using a noise generator is that the receiver electronics are operated at power levels equivalent to the galactic radio background at HF, closely mimicking an actual operating condition. See [P372] for plots of the galactic radio background noise temperature versus frequency.

Figure 1-3.a ~ A 50 ohm SMA-M termination is connected to the ANT 1 RF input of an RFSpace Cloud-IQ SDR receiver (termination is in lower-middle of image). The other connections are an Ethernet LAN cable and 5 Vdc power input cable. For the measurements in this paper, the associated SpectraVue software collects the output data from the receiver over the LAN and computes, displays and stores the continuum power within the preset frequency span, typically 10 or 20 MHz. Image © 2016 W. Reeve
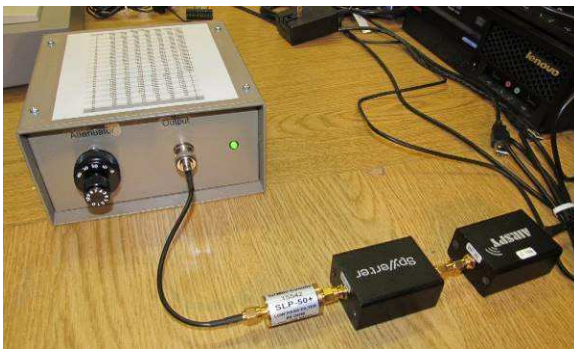

Figure 1-3.b ~ A HOT-1 noise generator (upper-left) is connected to the RF input of a SpyVerter up-converter and AirSpy SDR receiver combination through a 50 MHz lowpass filter (lower-right). The HOT-1 is set to a noise temperature of 46 300 K to mimic the galactic radio background at 20 MHz [P372, fig. 2]. The filter limits the noise bandwidth to reduce receiver overload. The AirSpy is connected by a USB cable to a Windows 10 PC (not shown). The SDR# software on the PC provides initial data processing and passes the data to Radio-Sky Spectrograph software for display and storage. For HOT-1 construction details see {HOT1}. Image © 2016 W. Reeve

The detected output will include the noise from the termination resistor or noise generator plus any noise added by the receiver. The receiver output will be stable to the extent that the receiver electronics, its power supply and environment are stable. If the receiver is placed in a temperature and humidity controlled environment, connected to a very stable power supply and allowed to warm up until all components are thermally stable, the output primarily will reflect the stability of the receiver electronics. Of course, this assumes the input is much more stable than the receiver; in any actual measurement the stability of the noise generator could affect the results. For purposes of this paper, the noise generators used in the measurements are assumed to have higher stability than the receiver and its environment, an assumption supported by the measurements discussed in Part II.

I-3. Output Fluctuations

When the receiver output noise power is expressed in terms of the system noise temperature, the output root-mean square (rms) fluctuation, or deviation, is given by

$$\sigma_{rms} \approx T_S \cdot (B \cdot \tau)^{-\frac{1}{2}} \tag{1}$$

where

σ_{rms} receiver rms output deviation (K)

T_S system noise temperature including the antenna noise temperature resulting from the received emissions (or noise generator), other noise within view of the antenna, and the receiver noise referred to its input (K)

B pre-detection bandwidth (Hz)

τ post-detection averaging (integration) time (s)

Equation (1) is the *ideal radiometer equation* for a total power receiver. The fluctuations due to the receiver's inherent characteristics can be reduced by increasing the bandwidth B or increasing the time τ or both. Reducing the fluctuations due to the receiver increases the system sensitivity because small noise temperature increases due to a weak radio source are less likely to be swamped by receiver noise. The integration time τ can be increased by increasing the response time of the smoothing filter on the detector output. Equivalently, because each sample of the output is not correlated with any other sample, taking the average of a block of n samples also increases τ . In this case $\tau = n \cdot \tau_0$, where τ_0 is the basic sampling interval. Using a block of samples modifies the ideal radiometer equation so that

$$\sigma_{rms} \approx T_S \cdot (B \cdot n \cdot \tau_0)^{-\frac{1}{2}} \tag{2}$$

During stability measurements the noise power T_S and receiver bandwidth B are fixed. The fixed components can be combined as a constant C_{fixed}, and the radiometer equation reduces to

$$\sigma_{rms} \approx C_{fixed} \cdot (n \cdot \tau_0)^{-\frac{1}{2}} \tag{3}$$

Therefore, the receiver output deviation σ_{rms} is proportional to the inverse square root of τ , or

$$\sigma_{rms} \infty (n \cdot \tau_0)^{-\frac{1}{2}} \tag{4}$$

Equation (4) is of the general form $y = x^a$, where in this case $x = n \cdot \tau_0$ and $a = -1/2$. If the logarithm is taken of a power-law relationship such as this, the result is $\log(y) = a \cdot \log(x)$. A plot of $\log(y)$ against $\log(x)$ on a graph with log-log scales will be a line with slope a. Similarly, when σ_{rms} from equation (4) is plotted on a log-log graph with respect to $n \cdot \tau_0$, the trace will be a straight line with slope $a = -1/2$ (figure 1-4). See **Appendix I-1** for

calculating the slope of a straight line on a log-log graph. The log-log plot is interpreted as follows: The deviation indicated by σ_{rms} decreases in a straight line as the number of samples n in the average increases. The decrease in σ_{rms} continues indefinitely if the noise involved is white FM noise or Gaussian. Non-Gaussian noise types exist and most do not reduce fluctuations through averaging. For example, flicker FM noise present in all electronic devices has a zero slope and fluctuations remain the same regardless of the amount of averaging. Random walk FM noise has a slope of +1 and the fluctuations increase with averaging. Random walk FM noise often is related to environmental conditions. See {Riley} for explanations of several power-law noise categories.
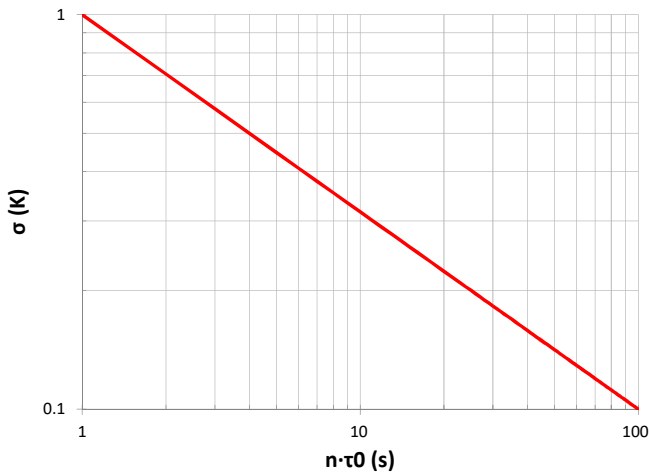

Figure 1-4 ~ Log-log plot of the output fluctuations from an ideal receiver with respect to the sampling interval $\tau_0 = 1$ s. The output follows the proportionality of equation (4) in which the noise deviation decreases as the number of averaged samples n increases from 1 to 100.

Non-Gaussian noise types always are present but they may not dominate white FM noise except during long averaging intervals. Therefore, the ideal radiometer equation can be closely approximated for short measurement intervals but impossible to achieve over long intervals. The definition of 'short' and 'long' depends on the receiver and can vary from seconds to hours as will be seen in Part II.

The output from practical systems is directly related to the receiver's overall power gain G and other factors, none of which are ever perfectly stable. It is convenient to assume that all imperfections are manifested as random gain fluctuations. The rms signal fluctuations due to such gain variations can be represented by

$$\sigma_G \approx T_S \cdot \left(\frac{\Delta G}{G} \right) \tag{5}$$

where ΔG is the rms gain fluctuations and G is the overall gain.

The random gain fluctuations and noise fluctuations are independent so their variances (squares of their rms deviations) are additive, thus

$$\sigma_T^2 = \sigma_{rms}^2 + \sigma_G^2 \approx T_S^2 \cdot \left[\frac{1}{B \cdot n \cdot \tau_0} + \left(\frac{\Delta G}{G} \right)^2 \right] \tag{6}$$

The total deviation is then

$$\sigma_T \approx T_S \cdot \left[\frac{1}{B \cdot n \cdot \tau_0} + \left(\frac{\Delta G}{G} \right)^2 \right]^{\frac{1}{2}}$$

(7)

The effects of gain variation can be reduced by a number of techniques. One is to rapidly cycle the receiver input between the antenna and a calibrated noise generator and then synchronously subtracting out the noise generator. The switching rate is set high enough so that the receiver gain does not change during the cycle. This is known as a *Dicke switch* after its inventor Robert Dicke. This technique and others alter the system sensitivity by a specific factor or constant K_S, thus, the ideal radiometer equation is changed to

$$\sigma_T \approx K_S \cdot T_S \cdot \left(B \cdot n \cdot \tau_0 \right)^{-\frac{1}{2}}$$

(8)

For the ideal radiometer, $K_S = 1$. Additional discussion of techniques to reduce gain variation effects is beyond the scope of this paper. For details, see chapter 7 in [Kraus] and chapter 6 in [Joardar].

Returning to the simple total power receiver, when the data averaging time is too long (block size too large) the output data starts to drift and shows non-random or systematic variations. These variations may be caused by cyclic or irregular changes in temperature, humidity or vibration, aging and instability of crystal oscillators or other components, heating of an internal CPU when under processing load that affects nearby components, internal power supply noise or slight output voltage variations in the external power supply, to name a few. Many of these causes are manifested as receiver gain variations; the causes of some may be identified, predicted and removed from the output data but others may be impossible to identify.

In the case of excessive averaging time – when non-Gaussian noise dominates – the simple proportionality of equation (4) is no longer valid and a log-log plot of the receiver output (with terminated input) deviates from a straight line with slope = –1/2. The point at which the line breaks from slope = –1/2 indicates the point (called the *knee*) when averaging or integration time is too long (figure 1-5). The slope of the line at various points on the plot can indicate the noise category, which may provide clues as to the process causing it. However, plots of real data usually include several noise processes and seldom are perfectly straight or have slopes corresponding to ideal power-law noise types for extended time periods, making them difficult to analyze.
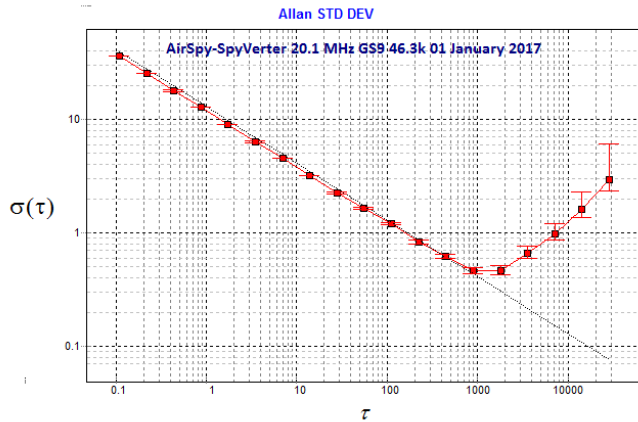
Figure 1-5 ~ Actual log-log plot of the output fluctuations from a software defined radio receiver that stops following the proportionality of equation (4) and breaks at an averaging time of 1000 s, where the "knee" is clearly visible. In this example, the noise in the output data can be reduced by averaging up to but not beyond 1000 s. Beyond 1000 s the deviation increases as more data is averaged. The data plot includes error bars. The downward sloping straight gray line overlaid on the data plot has a slope of − 0.5, the ideal condition for white FM noise.

I-4. Analysis

The output from a well-behaved receiver for short sampling intervals can be analyzed with the familiar statistics like Average and Standard Deviation. However, for long intervals both the Average and Standard Deviation associated with certain types of noise processes within receivers are proportional to the averaging time and never converge – the receiver output variations actually increase instead of decrease with averaging. The length of time when ordinary statistics fall apart varies with the receiver and can be measured as discussed in Part II.

When the ordinary Average and Standard Deviation cannot be used, a handy statistical tool for analyzing the receiver's output stability is the Allan Deviation $\sigma_y(\tau)$, which is a statistical function based on the sample interval τ (see {Allan}). The Allan Deviation converges for a greater variety of noise categories than the ordinary Standard Deviation. The Allan Variance (AVAR), which is the square of the Allan Deviation (ADEV), was originally introduced by David Allan at the National Bureau of Standards in the US in the mid-1960s for time and frequency measurements of extremely stable and accurate oscillators and clocks; however, it can be used to analyze any measurement taken as a continuous time series. The Allan Deviation assumes there are no dead times or gaps in the measurements.

Many modifications to the Allan Deviation have been developed for particular statistical conditions but they all share a common trait – the sum of the squares of the differences between adjacent values of the amplitude averages divided by various constants reflecting the number of samples involved. The Allan Deviation discussed here is the *overlapped variable tau estimator* {OVTE}, which is a general purpose form of the ADEV. It is called an estimator because it involves finite data sets (whereas ideal statistics involve infinite sets). It is equivalent to averaging the normalized samples in blocks of *n* samples (figure 1-6) prior to processing and is given by

$$\sigma_y\left(n\cdot\tau_0,N\right)=\left[\frac{1}{2\cdot n^2\cdot\tau_0^2\cdot\left(N-2\cdot n\right)}\cdot\sum_{i=0}^{N-2\cdot n-1}\left(x_{i+2\cdot n}-2\cdot x_{i+n}+x_i\right)^2\right]^{\frac{1}{2}} \qquad (9)$$

where

$\sigma_y\left(n\cdot\tau_0,N\right)$ Allan Deviation, abbreviated $\sigma_y\left(n\cdot\tau_0\right)$ in the rest of this paper

τ_0 data sampling interval

n integer multiplier for τ_0

N total number of samples in the data set
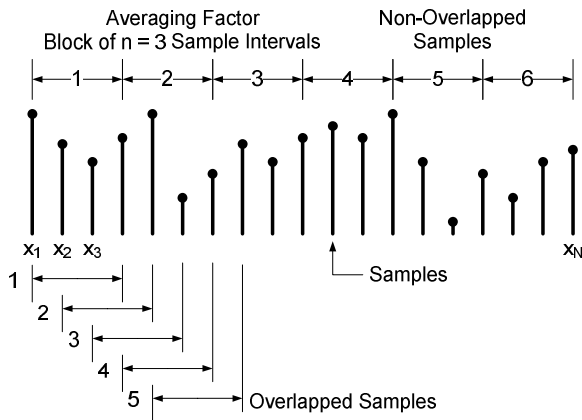
x_i sample value with index i

Figure 1-6 ~ Comparison of overlapped and non-overlapped sample averaging. Examples of non-overlapped samples are indicated by the callouts at the top and overlapped samples are indicated by the callouts at lower-left. For the non-overlapped samples, it is seen that the samples are broken into sequential groups for averaging purposes. On the other hand, overlapping uses samples from previous groups as they are averaged. The ADEV measurements and computations used in this paper use the overlapped samples. Adapted from {Riley}

The advantage of the overlapping Allan Deviation over other implementations is that it overlaps the samples for each averaging time and reduces the time to take measurements; however, the tradeoff is more computation. When computations involve white FM noise, the Allan Deviation is the same as the ordinary Standard Deviation; however, the Allan Deviation has the advantage of converging to a value that is independent of the number of samples when used with more divergent noise types such as flicker noise.

Note that equation (9) has two components. The left component is the divisor for normalizing and the right component provides a progression of averages that are added together for each *n* multiplier. To determine how $\sigma_y(n \cdot \tau_0)$ varies over any time period, *n* is assigned increasing integer values so that the intervals are $1 \cdot \tau_0$, $2 \cdot \tau_0$, $3 \cdot \tau_0$, ... , $n \cdot \tau_0$. For example, if the data is sampled every 0.1 s, then $1 \cdot \tau_0 = 0.1$ s, $2 \cdot \tau_0 = 0.2$ s, $3 \cdot \tau_0 = 0.3$ s, and so on. The computed values for $\sigma_y(n \cdot \tau_0)$ are plotted on a log-log-graph against $n \cdot \tau_0$.

Equation (9) can be setup in a spreadsheet for calculation (see **Appendix I-2** for a simple example). However, it is far more convenient to use a free software tool called ALAVAR {ALAVAR}; there also are Python software tools for computing the Allan Deviation (for example, {AllanTools}). ALAVAR computes and displays several types of the Allan Deviation. These are: 1) Overlapping Allan deviation ADEV; 2) Modified Allan deviation MDEV; 3) Overlapping Hadamard deviation HDEV; and 4) Time deviation TDEV. Only ADEV is used in this paper (figure 1-7). ALAVAR returns slightly different values than equation (9) but the results are equivalent. ALAVAR also provides plots of the original data values (figure 1-8) and power spectral density (PSD) of the data (figure 1-9) so that data can be visualized in the time and frequency domains. ALAVAR allows a high degree of plot customization.
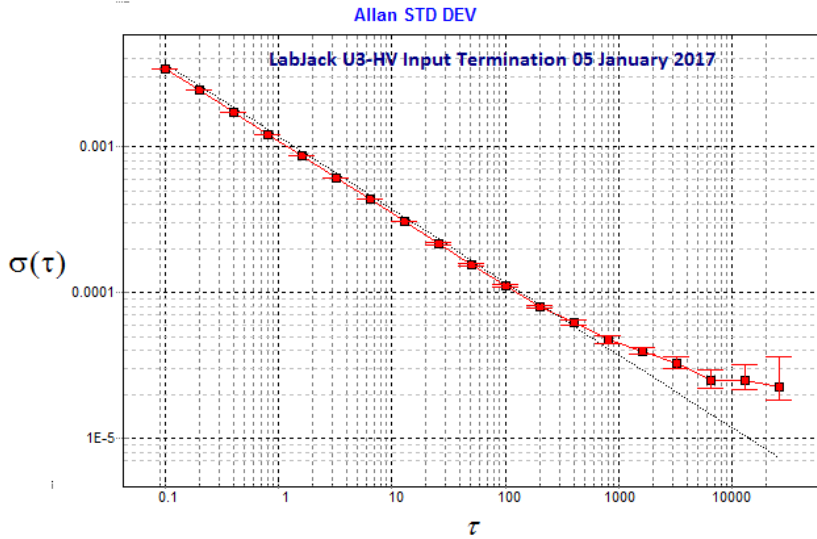
Figure 1-7 ~ Example ALAVAR plot of the Allan Deviation for a lab datalogger with τ_0 = 100 ms. The plot shows values of n from 1 to over 10 000. For these measurements, the datalogger single-ended input AIO0 was terminated with a 4.7k ohm resistor, and its output logged for 25 h. The trace closely corresponds to white FM noise out to about 1000 s (slope = –0.5) shown by the gray curve-fit line overlaid on the measurement trace. The noise continues to be close to white FM out to the end of the plotted averaging period of 25 000 s.
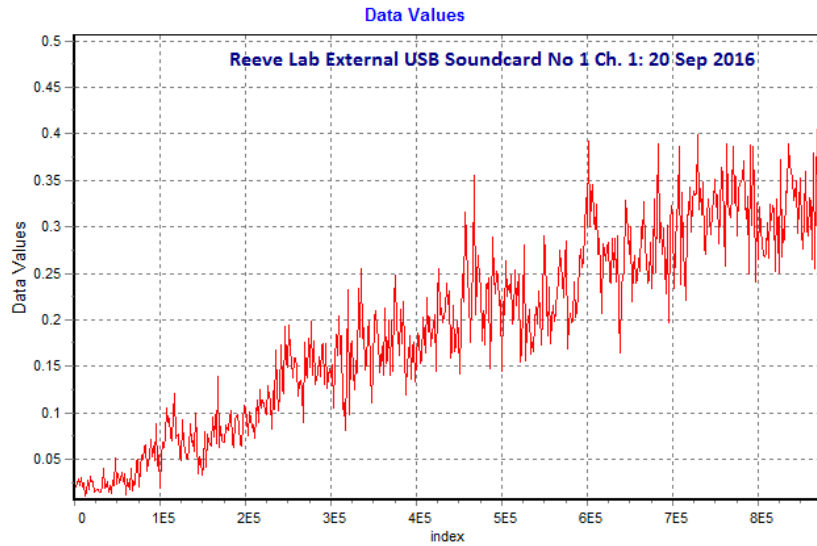

Figure 1-8 ~ Example ALAVAR plot of the amplitude data values in the time domain for a low performance external USB soundcard with its stereo Line Input terminated by 4.7k ohm resistors. The data shows an upward drift with time and obviously is not white FM noise. The Index axis is a count of the sample points, which are separated by 100 ms ($\tau_0 = 100$ ms). The data were collected for 25 h (900 000 samples).
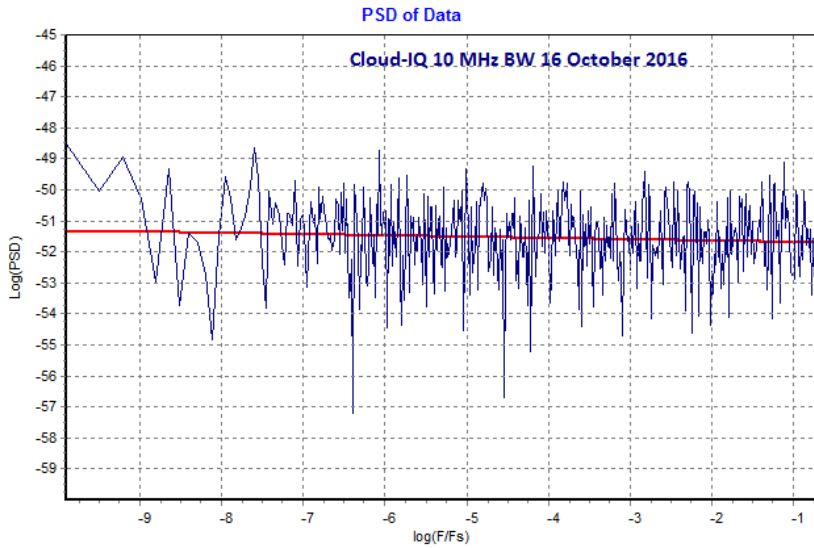
Figure 1-9 ~ Example ALAVAR plot of the power spectral density of the output from an RF sampling SDR receiver whose RF input is terminated with a 50 ohm termination. PSD is a measure of the output power intensity in the frequency domain and is computed from the FFT (fast Fourier Transform) spectrum of the data. The horizontal axis is frequency that is normalized to the sampling rate $F_S = 1/\tau_0$.

I-5. Acknowledgements

I am indebted to Wolfgang Herrmann, who's insightful and constructive comments immensely improved this paper.

I-6. References and Web Links

{Allan}   Allan, D., Statistics of Atomic Frequency Standards, Proceedings of the IRE, Vol. 54, No. 2, February 1966, available here: http://tf.boulder.nist.gov/general/pdf/7.pdf

{AllanTools}   https://pypi.python.org/pypi/AllanTools/2016.3

{ALAVAR}   http://www.alamath.com/

{HOT1}   http://www.reeve.com/Documents/Articles%20Papers/HOT-1Package_Reeve.pdf

[Joardar]   Joardar, S. and Claycomb, J., Radio Astronomy: An Introduction, Mercury Learning and Information LLC, 2016

[Kraus]   Kraus, J., Radio Astronomy, 2nd Ed., Cygnus-Quasar Books, 1986

[Monstein12]   Monstein, C., Allan Time, *Radio Astronomy*, May-June 2012

[Monstein14]   Monstein, C., Improving Long Time Stability of a Radio Astronomy Receiver, *Radio Astronomy*, March-April 2014

{OVTE}   https://en.wikipedia.org/wiki/Allan_variance

[P372]   ITU-R Recommendation P.372-13, Radio Noise, 2016, available here: http://www.itu.int/rec/R-REC-P.372/en

{Riley}   Riley, W., Handbook of Frequency Stability Analysis, National Institute of Standards and Technology, Special Publication 1065, July 2008, available here: tf.nist.gov/timefreq/general/pdf/868.pdf

Appendix I-1 ~ Slope on Log-Log Plot

The slope of a straight line on a log-log plot can be found from

$$Slope = \frac{\Delta \log Y}{\Delta \log X} = \frac{\log Y_2 - \log Y_1}{\log X_2 - \log X_1}$$

where
X_1, Y_1 and X_2, Y_2 are the points on the graph for which the slope is to be computed

Example:
Find the slope of the red line in the plot below.
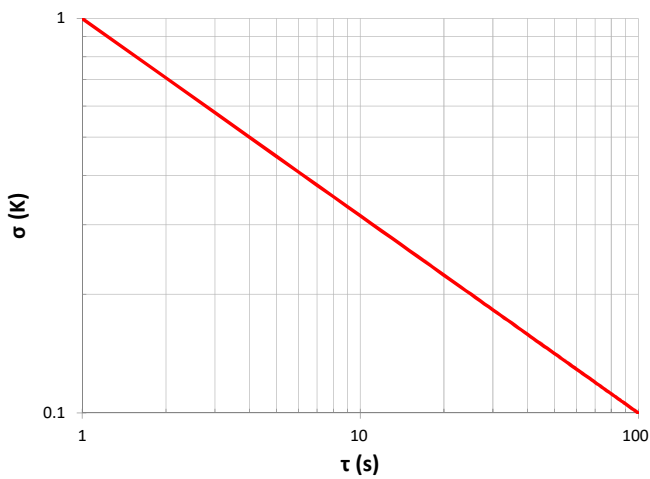
Solution:
$$x_1, y_1 = 1.0, 1.0$$
$$x_2, y_2 = 100.0, 0.1$$

$$Slope = \frac{\Delta \log Y}{\Delta \log X} = \frac{\log Y_2 - \log Y_1}{\log X_2 - \log X_1} = \frac{\log(0.1) - \log(1.0)}{\log(100.0) - \log(1.0)} = \frac{-1.0 - 0}{2.0 - 0} = -\frac{1}{2}$$

Appendix I-2 ~ Example ADEV Calculations

The overlapped ADEV estimator is used to compute ADEV for $\tau = n \cdot \tau_0$ where n = 1, 2, 3 and 4 using the N = 20 point time series directly below (x_0 through x_{19}). For n = 1, the original output data is used to calculate the summation (suffix in the equation). For n = 2, the previous calculation results for n =1 are used to calculate the summation, and so on. The time series was produced for this example by the random number generator is MS Excel 2010.

| x_i	Value	x_i	Value	x_i	Value	x_i	Value	x_i	Value
x_0	9.20	x_4	2.52	x_8	4.96	x_{12}	3.09	x_{16}	4.31
x_1	2.19	x_5	3.74	x_9	7.22	x_{13}	5.28	x_{17}	1.09
x_2	9.94	x_6	9.63	x_{10}	3.61	x_{14}	8.72	x_{18}	8.48
x_3	3.28	x_7	3.66	x_{11}	4.51	x_{15}	1.97	x_{19}	1.12

Allen Deviation: $\sigma_y(n \cdot \tau_0, N) = \left[\dfrac{1}{2 \cdot n^2 \cdot \tau_0^2 \cdot (N - 2 \cdot n)} \cdot \displaystyle\sum_{i=0}^{N-2 \cdot n-1} \left(x_{i+2 \cdot n} - 2 \cdot x_{i+n} + x_i \right)^2 \right]^{\frac{1}{2}} = \left(prefix \cdot \sum suffix \right)^{\frac{1}{2}}$

Index i	Output X_i	Prefix n=1	Suffix n=1	Prefix n=2	Suffix n=2	Prefix n=3	Suffix n=3	Prefix n=4	Suffix n=4
0	9.20	0.027778	217.8576	0.007813	66.5856	0.003968	150.5529	0.002604	83.1744
1	2.19		207.6481		0.3969		0.6561		3.7249
2	9.94		34.8100		211.1209		55.0564		32.6041
3	3.28		3.9204		0.2916		76.7376		0.2209
4	2.52		21.8089		138.7684		1.4161		18.5761
5	3.74		140.6596		13.2496		2.7889		29.3764
6	9.63		52.8529		11.0224		2.9584		123.8769
7	3.66		0.9216		39.3129		2.9584		11.4921
8	4.96		34.4569		0.6889		21.7156		9.5481
9	7.22		20.3401		12.1104		9.0601		5.0625
10	3.61		5.3824		37.8225		6.9696		28.6225
11	4.51		13.0321		16.6464		140.1856		2.8561
12	3.09		1.5625		100.8016		58.2169		
13	5.28		103.8361		5.9049		4.9284		
14	8.72		82.6281		73.6164				
15	1.97		30.9136		0.8281				
16	4.31		112.5721						
17	1.09		217.5625						
18	8.48								
19	1.12								

Sum	20.00	0.027778	1302.77	0.007813	729.17	0.003968	534.20	0.002604	349.14
n		1		2		3		4	
AVAR		36.1879		5.6966		2.1198		0.9092	
ADEV		6.01564		2.38676		1.455969		0.953523	

Summary:

n	ADEV	AVAR
1	6.0156	36.1879
2	2.3868	5.6966
3	1.4560	2.1198
4	0.9535	0.9092

Average slope of ADEV plot = −1.33
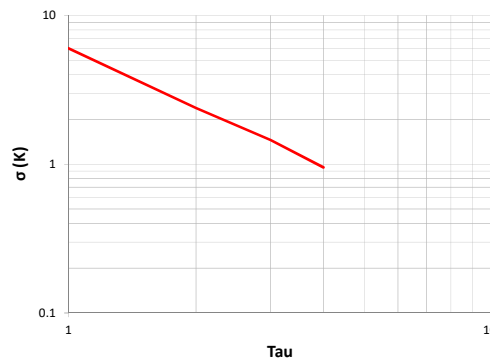
Document information

Author: Whitham D. Reeve

Copyright: © 2017 W. Reeve

Revision: 0.0   (Original draft started for Callisto, 09 Nov 2012)

           0.1   (Rewrite for general HF application, 10 Sep 2016)

           0.3   (Define AVAR, 13 Sep 2016)

           0.4   (Add receivers and rewrote sect. 2, 17 Sep 2016)

           0.5   (Add Dicke switch and soundcard measurements, 20 Sep 2016)

           0.6   (Split into two parts, 20 Sep 2016)

           0.8   (Rework sections 1-1 and 1-2, 01 Oct 2016)

           0.9   (Rework sections 1-1 and 1-2 again, 09 Oct 2016)

           1.0   (Add noise generator termination, 29 Oct 2016)

           1.1   (Released for review and comment, 05 Nov 2016)

           1.2   (Incorporated W. Herrmann comments, 18 Nov 2016)

           1.3   (Incorporated W. Herrmann comments, 21 Jan 2017)

           1.4   (Finalized, 17 Feb 2017)

           1.5   (Changed title to include 'output', 21 Mar 2017)

Word count: 4310

File size: 500224